

A Functional Protein Chip for Combinatorial Pathway Optimization and *In Vitro* Metabolic Engineering

Gyoo Yeol Jung and Gregory Stephanopoulos,
Department of Chemical Engineering
Massachusetts Institute of Technology, Cambridge, MA 02139

Abstract— Pathway optimization is, in general, a very demanding task due to the complex, nonlinear and largely unknown interactions of enzymes, regulators and metabolites. While *in vitro* reconstruction and pathway analysis is a viable alternative, a major limitation of this approach is the availability of the pathway enzymes for reliable pathway reconstruction. Here, we report the application of RNA display methods for the construction of fusion (chimeric) molecules, comprising mRNA and the protein they express, that can be used for the above purpose. The chimeric molecule is immobilized via hybridization of its mRNA end with homologous capture DNA spotted on a substrate surface. We show that the protein (enzyme) end of the fusion molecule retains its function under immobilized conditions and that the enzymatic activity is proportional to the amount of capture DNA spotted on the surface of a microarray or 96-well microplate. The relative amounts of all pathway enzymes can thus be changed at will by changing the amount of the corresponding capture DNA. Hence, entire pathways can be reconstructed and optimized *in vitro* from genomic information alone by generating chimeric molecules for all pathway enzymes in a single *in vitro* translation step and hybridizing on 96-well microplates where each well contains a different combination of capture DNA. We provide validation of this concept with the sequential reactions catalyzed by luciferase and nucleoside diphosphate kinase and further illustrate this method with the optimization of the five-step pathway for trehalose synthesis. Multi-enzyme pathways leading to the synthesis of specialty molecules can thus be optimized from genomic information about the pathway enzymes, provided the latter retain their activity under the *in vitro* immobilized conditions..

Index Terms—functional protein chip, *in vitro* metabolic engineering, combinatorial pathway optimization, trehalose synthesis.

I. INTRODUCTION

The properties of metabolic pathways uniquely depend on the relative activities of all the enzymes that they comprise. As such, metabolic pathways can be optimized by manipulating the relative expression of the corresponding

This work was supported by the DuPont-MIT Alliance and the Singapore-MIT Alliance.

G. Y. Jung is with Department of Chemical Engineering, Massachusetts Institute of Technology, Room 56-422, Cambridge, MA 02139 (phone: 617-253-6591, e-mail: gyjung@mit.edu).

G. Stephanopoulos is with Department of Chemical Engineering, Massachusetts Institute of Technology, Room 56-469, Cambridge, MA 02139 (corresponding author to provide phone: 617-253-4583, e-mail: gregstep@mit.edu).

genes such as to maximize the amount of a specialty product that they synthesize or to minimize an undesirable metabolite associated with disease. Pathway optimization through the introduction of genetic controls is indeed a central tenet of metabolic engineering¹. However, despite recent advances in pathway optimization and metabolic engineering²⁻⁵, this remains a very demanding undertaking due to the complexity of metabolic pathways and the difficulty in obtaining sufficient measurements about the intracellular environment. Popular methods, such as single gene over-expression or over-expression of *all* pathway genes, are optimal strategies only in special cases, suggesting the need for a holistic approach to this problem. Mathematical theories are sufficiently developed to yield rational solutions to pathway optimization provided that satisfactory kinetic models are available for the pathway reactions. However, their use has been rather limited exactly because reliable models of *in vivo* pathway function are mostly unavailable. As a result, pathway optimization must rely on experimental methods of combinatorial search nature, whereby the relative amounts (or activities) of the pathway enzymes are altered and the effect on the pathway performance is measured. In principle, this would be a viable option, especially in light of recent advances in the miniaturization of experimental searches of this type⁶⁻⁹, except for the general enzyme unavailability in pure and active form for reconstructing the pathway of interest.

mRNA-protein fusions, originally developed for use in RNA display¹⁰, are molecules linking covalently an expressed mRNA and its translated protein product. As such, these fusion molecules (Fig. 1a) comprise two distinct parts. One, (mRNA), carrying genetic information that can be used as unique and specific tag complement for capturing the fusion molecule by a homologous capture DNA, and another (protein) that is endowed with potential functionality. If the capture DNA is immobilized on a solid support, it could be used as anchor for attaching the entire chimeric molecule on the support. The specificity of the mRNA-DNA hybridization suggests that a particular chimeric molecule could be recognized in a mixture of similar molecules and specifically attached to a particular space of a solid support (Fig. 1b). In this case, the number of fusion molecules immobilized should be proportional to the amount of DNA capture molecules attached on the support. Once a fusion molecule is immobilized by hybridization, the protein end of it would be available for carrying out its usual functions provided that it retained its activity under

II. MATERIALS AND METHODS

A. Preparation of mRNA-protein fusion molecules

mRNA-protein fusion molecules were synthesized by the method reported by Roberts and Szostak¹⁰ with a modification. Each RNAs were splint-ligated to the puromycin-oligo DNA linker [5'-d(A27CC)-P] possessing a 5'-phosphate and a 3'-puromycin by T4 DNA ligase (P in the above sequence denotes puromycin). Ligation products were purified by gel extraction and *in vitro* translated in rabbit reticulocyte lysate system purchased from Ambion (Austin, TX). After 90 min translation, the reaction mixture was adjusted to 150 mM MgCl₂ and 425 mM KCl to promote the formation of the puromycin-peptide bond.

B. Preparation of functional protein chip

Proper amounts of capture DNAs designed for specific, non-interacting sequences along the target RNAs were spotted on poly-lysine coated surface of 96-microwell plate (BD Biosciences Clontech, Palo Alto, CA) and crosslinking was carried out under UV light in UV crosslinker (Stratagene, La Jolla, CA). Capture DNA molecules were synthesized from Integrated DNA Technologies Inc. (Coralville, IA) as follows:

luciferase : 5'AGCCTTATGCAGTTGCTCTC3'
ndk : 5'TCTCTTTCAGCACTTTCCTT3'
udpgp : 5'GCGCTGCTCAAGGAGTGATT3'
hxl1 : 5'CAACTTTTCGATATCGGAAA3'
pgm : 5'CGTCTTTATCAAGGTGCATA3'
otsA : 5'CAAGAACGCCCGGATTGGCT3'
otsB : 5'TCACCTTTACTGGTACCTCT3'

A mixture of mRNA-protein fusion molecules is synthesized in a single vial by *in vitro* transcription-translation. The mixture is subsequently applied to microplate wells whose surface contains capture DNA molecules. Following prehybridization with 1 % ultra-pure bovine serum albumin (Ambion, Inc., Austin, TX), fusion molecules are specifically hybridized with their corresponding capture DNA molecules. Residual fusion molecules are washed out from the well by washing twice with 1X PBS buffer (pH 7.6). After refreshing with a proper reaction buffer in the well, the enzymes immobilized on the surface are ready to catalyze the reaction. The relative amounts of capture DNA molecules immobilized on the surface of the wells determine the relative activity of the enzymes in the well.

C. Enzymatic Reactions

A sequential reaction catalyzed by nucleoside diphosphate kinase (NDK) and luciferase was carried out based on the method developed by Karamohamed *et al.*¹² 50 μ l of reaction buffer containing the following components: 0.1 M Tris-acetate (pH 7.75), 2 mM EDTA, 10 mM magnesium acetate, 0.1 % BSA, 1 mM dithiothreitol (DTT), 0.4 mg/ml polyvinylpyrrolidone (360,000), 100 μ g/ml D-luciferin. Reaction was performed at room temperature for 1 hr and the resulting luminescence was measured by FusionTM microplate

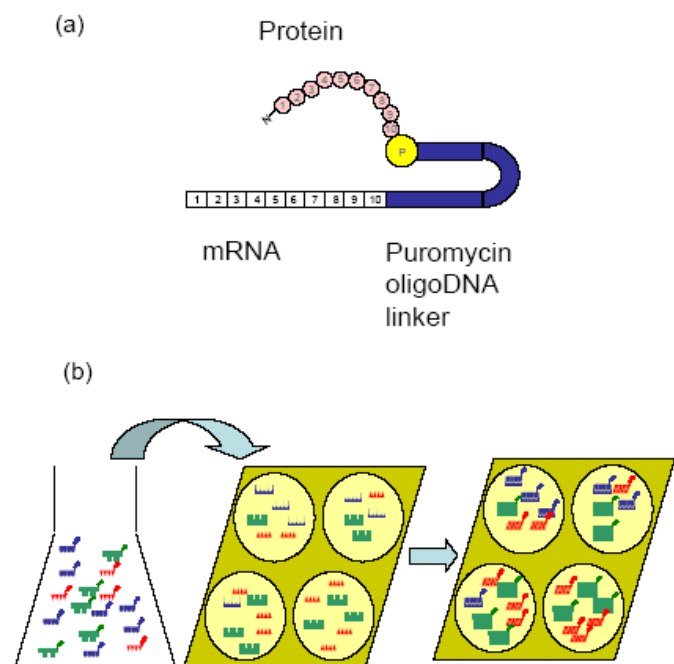


Fig. 1. (a) Schematic of the mRNA-protein fusion molecule used for RNA display applications and employed in this study. mRNA-protein fusion molecules were synthesized by *in vitro* translation system derived from rabbit reticulocyte. (b) Illustration of the method employed in the construction of functional protein chips using mRNA-protein fusion chimeras and their homologous capture DNA molecules

immobilized conditions.

Weng *et al.*¹¹ recently demonstrated that mRNA-protein fusion molecules could be hybridized on a DNA microarray to build a protein microarray. Using three different types of proteins and their tagged antibodies it was shown that mRNA-protein fusion molecules could specifically bind to their corresponding capture DNA. In this study, we employed this platform for catalytically active proteins in order to reconstruct metabolic pathways whose enzymes were not readily available. A novel feature of this work is the parallel generation of all mRNA-enzyme fusion molecules in a single *in vitro* translation step. The relative amounts of the different types of fusion molecules immobilized on the wells of a 96-well microplate were controlled by the amounts of unique capture DNA molecules designed for each target enzyme. A key finding is that all seven mRNA-enzyme fusions examined retained their catalytic activity under immobilized conditions. The main result is that this arrangement facilitated the experimental investigation of numerous combinations of relative enzyme activities and ultimately the optimization of the five-step pathway for trehalose synthesis. Other combinations of relative enzyme activities were clearly suboptimal yielding inferior overall pathway performance.

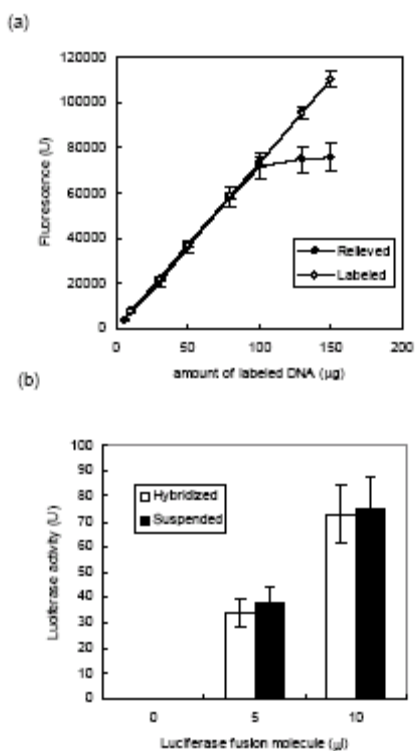


Fig. 2. The efficiency of crosslinking and hybridization. (a) Crosslinking efficiency. Fluorescein-labeled luciferase capture DNA was crosslinked in UV crosslinker as described in Materials and Methods. Fluorescence was measured by Fusion™ microplate reader (Perkin Elmer, Co., Wellesley, MA). Arbitrary unit was used for fluorescence. (b) Hybridization efficiency. Hybridization process was carried out in the well with 5 µg of luciferase capture DNA described in Materials and Methods. For the suspended version, same hybridization process was carried out on the well without capture DNA to avoid the effect of hybridization process. After hybridization, luciferase activities were measured under the condition described in Materials and Methods.

reader (Perkin Elmer, Co., Wellesley, MA). One light unit defined as an amount of enzyme producing a biometer peak height equivalent to 0.02 µCi of ^{14}C in PPO/POPOP cocktail. Light units measured in 50 µl assay mixture containing 5 µmol ATP and 7.5 µmol luciferin in Tris-glycine buffer, pH 7.6, at 25 °C. The correlation between the light unit and luminescence was determined by using the authentic luciferase purchased from Sigma-Aldrich (St. Louis, MO).

Trehalose synthesis was carried out in the buffer containing 50 mM Tris-Cl (pH 7.6), 10 mM magnesium chloride, 110 mM glucose, 55 mM ATP, 16.7 mM UTP, and 16.7 µg/ml glucose-1,6-bisphosphate for 3 hr at 30 °C. Synthesized trehalose was measured using the method with acid trehalase¹³.

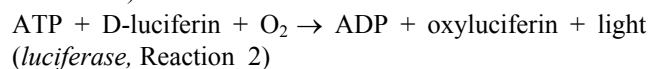
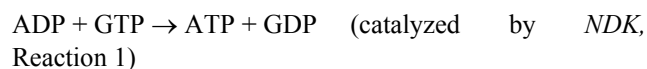
A. Efficiency of capture DNA crosslinking

Fluorescein-labeled oligonucleotides coding luciferase capture DNA synthesized from Integrated DNA technologies, Inc. (Coralville, IA) were loaded on the well coated by poly-lysine and crosslinking was carried out in the UV crosslinker (Stratagene, La Jolla, CA). After crosslinking, wells were washed twice with 200 µl of 1X PBS solution and negligible fluorescence was found from the washed solution up to 100 µg. However, slight fluorescence from washed solution was observed over 100 µg of DNA. This indicates that poly-lysine coated microwell can immobilize up to 100 µg of DNA. Fluorescein tags were relieved from the surface by treating DNase and measure their fluorescence compared with the same amount of fluorescein-labeled capture DNA loaded (Fig. 2a). Almost 100 % crosslinking efficiency can be found up to 100 µg and DNA was saturated at 100 µg.

The activity of hybridized luciferase fusion molecule was compared with that of suspended one (Fig. 2b). In order to avoid the effect of hybridization, luciferase fusion molecules were loaded on the well free from capture DNA and carried out the same hybridization process as described in Materials and Methods. The activities of the hybridized fusion molecules on the surface were found as similar with the equivalent amount of fusion molecules in the solution, which indicated that the immobilization does not affect on the activity of fusion molecules.

B. A sequential reaction by NDK and luciferase

We first sought to validate the basic premises of this approach, i.e., (a) that chimeric molecules hybridize on homologous DNA attached to a solid support, (b) that the enzyme end of the chimera retains its activity when attached to the support, and, (c) that enzymatic activity is proportional to the amount of capture DNA spotted on the solid support. The sequential reaction catalyzed by nucleotide diphosphate kinase (NDK) and luciferase was used for this purpose as a model system¹²:



mRNA-enzyme fusion molecules were synthesized in the modified *in vitro* translation system from rabbit reticulocyte lysate and were loaded on the wells of a 96-well microplate each containing different amounts of DNA capture molecules for the two enzymes, NDK and luciferase as described in Materials and Methods.

Fig. 3 summarizes the results obtained when different amounts of a particular type of capture DNA in the wells were used with different volumes of load solution obtained from the *in vitro* translation of *individual* fusion molecules (henceforth

termed “solution”). For the same solution volume (i.e., same amount of fusion molecules), Fig. 3a shows that the activity of each reaction increases and then saturates as the amount of capture DNA spotted on the wells increases. Apparently 0.3 μg of capture DNA is sufficient to hybridize all fusion molecules produced by *in vitro* translation of luciferase or NDK. When the amount of capture DNA is fixed at the maximum of 0.3 μg , the activity of each enzyme increases linearly (up to 40 μl of solution) with the amount of solution loaded on the well, (Fig. 3b). Next, we wished to investigate the specificity of hybridization when fusion molecules of *both enzymes* were present in the solution. To this end, mixtures of fusion molecules (all translated in a single step) were loaded on wells containing different combinations of the two types of capture DNA. Fig. 3c shows the activity of luciferase in wells containing varying amounts of luciferase capture DNA molecule and the same amount (0.3 μg) of NDK capture DNA. Similarly, Fig. 2d shows the activity of NDK in wells containing

varying amounts of NDK capture DNA and the same amount (0.3 μg) of luciferase capture DNA. In both cases the same amount of solution was used containing both types of fusion molecules. The linear dependence seen in both cases is evidence for the *specificity* of the hybridization between fusion molecules and capture DNA, as well as the activity of each fusion enzyme of the consecutive reaction system of equations (1) and (2). A replica set of reactions with RNase-treated fusion molecules showed no activity at all, evidence of the critical role played by the mRNA portion of the fusion molecule in capturing the enzymatic activity.

The above results demonstrate the two advantages of the described approach. First, reaction mixtures containing *all types of fusion molecules* can be directly applied to the well without any purification. Only a single step of *in vitro* translation is required to generate all fusion molecules that are subsequently separated by specific hybridization in amounts (and locations) controlled by the homologous capture DNA

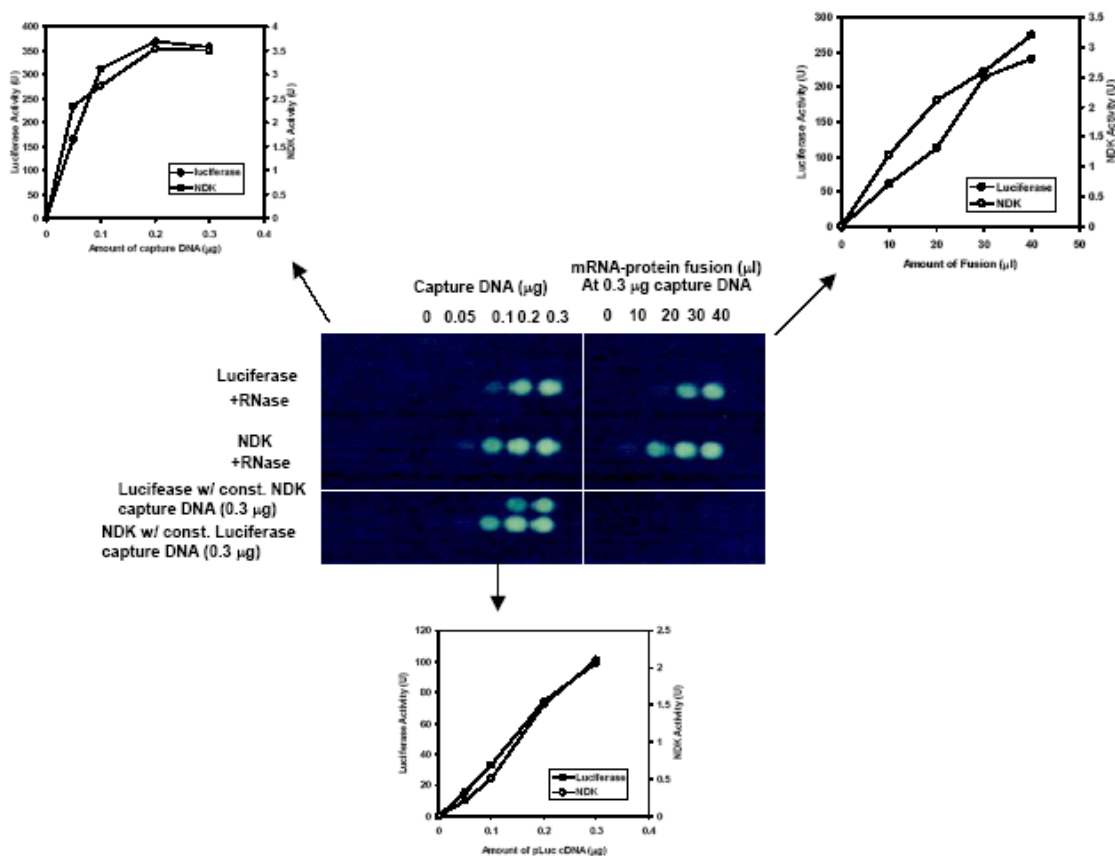


Fig. 3. Activity and specificity of the mRNA-Enzyme chimeras immobilized by homologous recombination with capture DNA molecules attached on a microwell surface. The sequential reaction of luciferase and nucleoside diphosphate kinase (NDK) was used as test system: (a) Effect of increasing amounts of capture DNAs on enzymatic activities. 30 μl of fusion molecules solution were loaded in each well. (b) Effect of increasing amounts of fusion molecules on enzymatic activities with 0.3 μg of capture DNA molecules spotted on each well. (c) Specificity of hybridization between fusion molecules and capture DNA. Mixtures of fusion molecules (all translated in a single step) were loaded on wells containing different combinations of the two types of capture DNA. Shown are the activity of luciferase in wells containing varying amounts of luciferase capture DNA molecule and the same amount (0.3 μg) of NDK capture DNA and the activity of NDK in wells containing varying amounts of NDK capture DNA and the same amount (0.3 μg) of luciferase capture DNA. In both cases the same amount of solution was used containing both types of fusion molecules. Closed and open symbols represent luciferase and NDK, respectively.

molecules. Second, processing time is minimized for immobilizing the enzymes on supports at numerous combinations suitable for high throughput testing.

C. Optimization of trehalose synthesis pathway

While the two-step pathway of reactions (1) and (2) yielded encouraging results, for broader use, it is necessary that the applicability of the above platform be demonstrated with a realistic pathway exhibiting the network and regulatory complexities present in real metabolic bioreaction networks. To this end, we selected the trehalose synthesis pathway from glucose (Fig. 4h). Trehalose is a disaccharide with a large potential market as a multi-functional sweetener, moisture retainer in cosmetics and preservative in pharmaceutical products and frozen foods, among others.¹⁴ It is synthesized in

yeast and has also been observed in bacterial fermentation products.^{15,16} The pathway of trehalose synthesis harbors a branch point (glucose-6-phosphate) where flux distributions between two competing reactions can materially impact end-product accumulation. Additionally, very little is known about the kinetics and regulation of the five reactions of the pathway, only one of the enzymes is commercially available, and overabundance of any single enzyme or all five together does not yield an optimal system in terms of maximal trehalose accumulation rate. It is therefore of interest to determine the optimal profile of relative enzymatic activities, or relative gene expression rates for an *in vivo* application, that would maximize the rate of this pathway.

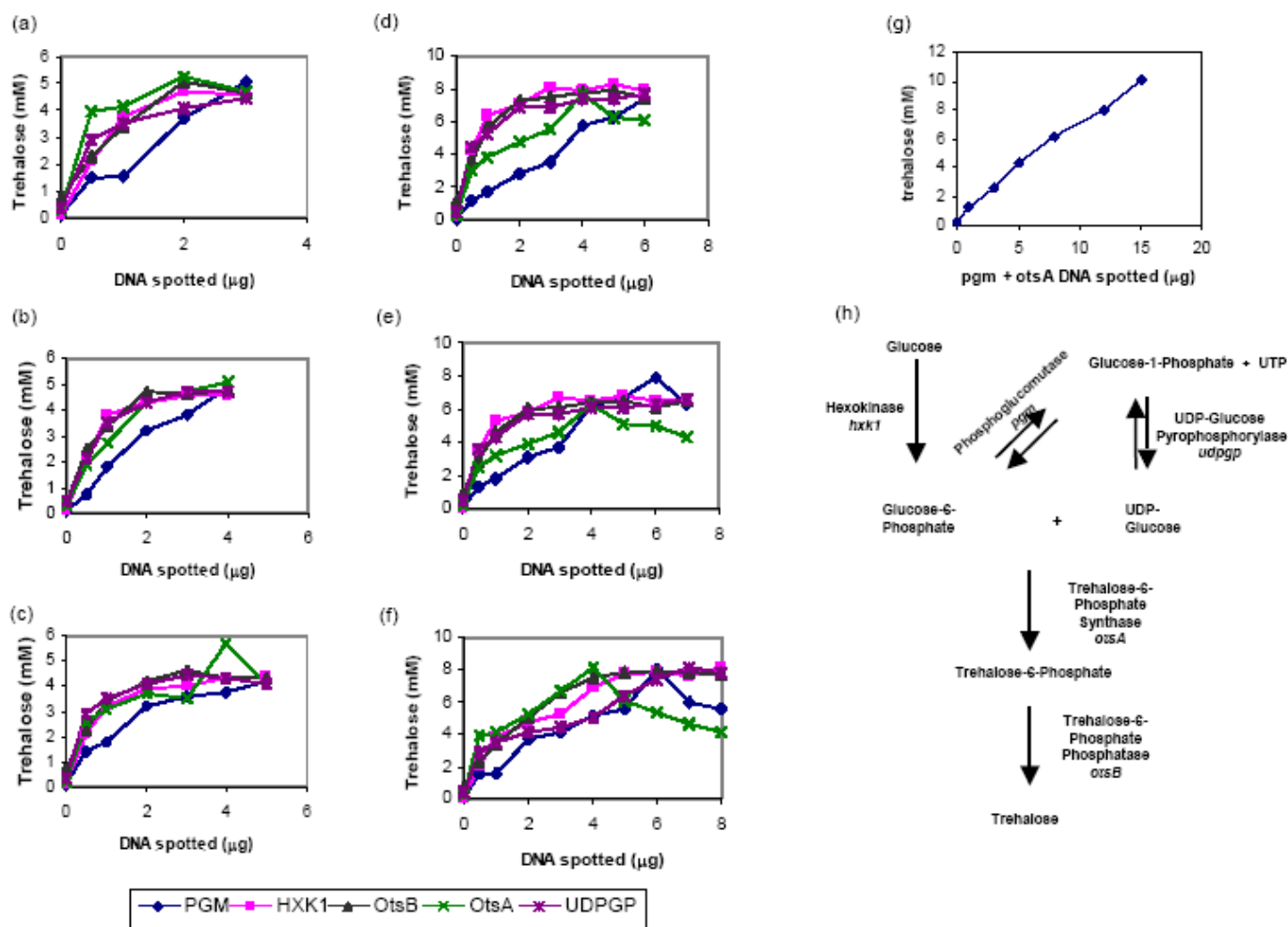


Fig. 4. Systematic optimization of the trehalose synthesis pathway using the functional protein chip of this study. Total trehalose was determined at 3 hr after initiation of reaction (23). The effect of varying amounts of each pathway enzyme on trehalose synthesis was examined while keeping the other enzymes fixed at (a) 3 μg , (b) 4 μg , and (c) 5 μg based on capture DNA molecules. As the optimal amount of OtsA was determined at 4 μg , further experiments were carried out with 4 μg of OtsA while the other enzymes were fixed at the levels of, (d) 6 μg and (e) 7 μg in terms of capture DNA molecules. (f) Effect of varying enzyme amounts on trehalose synthesis under the optimal condition (4 μg of OtsA and 6 μg of PGM) with the other enzymes were set at 8 μg in terms of capture DNA. (g) Amount of trehalose product synthesized for varying amounts of total PGM and OtsA maintained at the optimal ratio of 3/2. Other enzymes were saturated at 8 μg based on capture DNA in each reaction mixture. (h) Schematic of the trehalose synthesis pathway used in this study. All the genes were cloned from the *E. coli* K12 genomic DNA except for *hvk1* cloned from *Saccharomyces cerevisiae* by polymerase chain reaction using the primers described in Table I.

TABLE I
PRIMERS USED FOR PCR TO CLONE THE GENES IN TREHALOSE SYNTHESIS
PATHWAY

Gene	Primers
<i>udpgp</i>	Psense: 5'ATGACGAATTTAAAAGCAGT3'
	Pantisense: 5'GAGCTCTTATTCGCTTAACAGCTTCT3'
<i>hxx1</i>	Psense: 5'ATGGTTCATTTAGGTCCAAA3'
	Pantisense: 5'AGTACTAGCGCCAATGATACCAAGAG3'
<i>pgm</i>	Psense: 5'ATGGCAATCCACAATCGTGC3'
	Pantisense: 5'GAGCTCCGCGTTTTTCAGAACTTCGC3'
<i>otsA</i>	Psense: 5'ATGAGTCGTTTAGTCGTAGT3'
	Pantisense: 5'AGTACTCGCAAGCTTTGGAAAGGTAG3'
<i>otsB</i>	Psense: 5'GTGACAGAACCGTTAACCGA3'
	Pantisense: 5'AGTACTATACTAACGACTAAACGACTC3'

In lieu of a complete combinatorial search, we systematically explored the kinetics of the trehalose pathway as follows: First, we examined the effect of each enzyme on trehalose synthesis by setting the amounts of all but one enzyme at a constant level and measuring the rate of trehalose synthesis as the amount of the enzyme of interest was increased from zero to the same level as the other four enzymes (We did not actually measure the activities of the five enzymes; their actual amounts and activities were controlled by the amount of the corresponding homologous capture DNA that was spotted on the well of the 96-well microplate.). This was done with each of the five pathway enzymes and the entire process was repeated for a higher enzyme level. Each curve in Fig. 4a shows the amount of trehalose synthesized over a 3-hour period when the amounts of all but one enzyme are set at the maximum captured by 3 μg of spotted capture DNA and the amount of the fifth is varied between 0 and 3 μg . Figs. 4b and 4c show the trehalose amounts obtained in similar experiments where the maximum enzyme amounts were set by 4 μg and 5 μg of capture DNA, respectively. It can be seen that, while saturation profiles are obtained for the lower enzyme amounts, a trehalose synthesis rate maximum is observed, (Fig. 4c), when the maximum enzyme is set by 5 μg of capture DNA for all four enzymes except trehalose-6-phosphate synthase (OtsA). The maximum trehalose synthesis rate occurs when OtsA is at the amount determined by 4 μg of OtsA capture DNA. Figs. 4d and 3e show the product amounts obtained when OtsA is set by the optimum of 4 μg of its capture DNA and the amount of the other enzymes is similarly increased to 6 μg and 7 μg of capture DNA, respectively. In these graphs, trehalose productions are found to be elevated compared to the previous one shown in Fig. 3c from three curves corresponding to hexokinase

(HXK1), UDP-glucose pyrophosphorylase (UDPGP) and trehalose-6-phosphate phosphatase (OtsB). In these three cases, the level of OtsA was set by 4 μg of capture DNA yielding the maximum trehalose production which seemed to enhance the trehalose flux even for the low concentration range. The optimized OtsA, however, did not affect the curve for PGM, and this can be evidence that PGM is another limiting step for trehalose production. We observe that, while a monotonic response is obtained for the three enzymes of hexokinase (HXK1), UDP-glucose pyrophosphorylase (UDPGP) and trehalose-6-phosphate phosphatase (OtsB), the trehalose amount is maximized at 6 μg of capture DNA for phosphoglucosyltransferase (PGM) (Fig. 4e). Each curve in Fig. 3f shows the trehalose product obtained when the amount of the corresponding enzyme is varied between 0 and 8 μg while the three enzymes, HXX1, UDPGP and OtsB are kept at the maximum of 8 μg of capture DNA, and OtsA and PGM are set at the optimal levels captured by 4 and 6 μg of spotted DNA respectively. In summary, for the enzyme levels examined, increasing the amounts of the three enzymes, e.g., HXX1, UDPGP, and OtsB, enhances trehalose synthesis as evidenced by the monotonic increase of the trehalose amounts obtained with increasing amounts of the corresponding capture DNA. On the other hand, PGM and OtsA have optimal activities at which they must be maintained for maximum trehalose synthesis.

We note that PGM and OtsA are enzymes at the branch point of the pathway and maintaining an optimal balance of their activities is the key for optimal flux allocation. Too high of PGM activity will drain the pool of glucose-6-phosphate required in the condensation reaction catalyzed by OtsA. Similarly, too high activity of OtsA cannot be supported by the available pool of UDP-Glucose unless an optimal activity of PGM is also present. As shown in Figs. 3a and 3b, no optimal amounts of PGM and OtsA are found, indicating that, at these levels, the activities of both enzymes were too low to deplete the pool of glucose-6-phosphate. Throughout all experiments conducted with various enzyme amounts (Fig 4c – 4f), trehalose synthesis is maximized when the three enzymes (HXK1, UDPGP and OtsB) are maintained at maximum activity while the activity of PGM and OtsA is controlled at the optimal ratio of 3/2. This finding was tested in a subsequent experiment in which the total amount (and therefore activity) of PGM and OtsA was varied from 0 to 15 μg while maintaining the optimal ratio of 3/2 and with the other three enzymes saturated at 8 μg of capture DNA. As seen in Fig. 3g, the trehalose synthesis rate increases linearly with the total amount of *pgm* and *otsA* capture DNA (at the 3/2 ratio). This result demonstrates the elimination of pathway kinetic limitations by maintaining an optimal profile of enzymatic activities.

Trehalose 6-phosphate is known to inhibit hexokinase in *Saccharomyces cerevisiae*,¹⁷⁻¹⁹ and this could explain in part the observed results: Increasing OtsA activity leads to trehalose 6-phosphate accumulation that would, in turn, cause reduction

of the production of glucose 6-phosphate and overall pathway flux. This effect alone, however, cannot explain the observed effects of PGM on the flux or the fact that decreased trehalose synthesis is seen at increased OtsB activities. A complete explanation of the observed pathway kinetics should be sought in an overall flux distribution model derived from individual enzymatic kinetics and regulation. It is nevertheless of interest to observe that the trehalose synthesis rate increases linearly with the total amount of PGM and OtsA enzymes, as long as their balance is maintained at the optimal ratio of 3/2. By fixing the relative enzyme activities around the branch point, the whole pathway can be regarded as an independent *linear* pathway whose flux increases linearly with the activity of the pathway enzymes according to Kacser's "Universal Theorem."²⁰

IV. CONCLUSION

While the focus of this research was on metabolic pathway optimization, the chimeric molecules of RNA display can have much broader applications. Immobilization of functionally active proteins that are usually unavailable but can be obtained from genomic information by *in vitro* translation is of importance in the manufacturing of microarrays for protein capture for analytical applications (protein microarrays),^{8,9} screening of protein libraries for binding to target molecules, and screening of peptides or natural products for inhibition of binding activity. We also envision applications for the production of high added value compounds by reconstructing entire pathways for the synthesis of such compounds. Examples include proteins with specific glycosylation patterns and other post-translational modifications and reactions, in general, catalyzed by unavailable enzymes that can be produced *in vitro* from their genomic sequence and conveniently immobilized using their capture DNA homologue. A particular advantage of the described method is the *parallel* synthesis of many chimeric molecules by *in vitro* translation of all such molecules at the same time. The specificity of immobilization by the homologous capture DNA molecules simplifies drastically the many purification steps that would be needed otherwise.

REFERENCES

- [1] G. Stephanopoulos and J. J. Vallino, "Network rigidity and metabolic engineering in metabolite overproduction.," *Science*, vol. 252, pp. 1675-1681, 1991.
- [2] W. R. Farmer and J. C. Liao, "Improving lycopene production in *Escherichia coli* by engineering metabolic control," *Nat. Biotechnol.*, vol. 18, pp. 533-537, 2000.
- [3] W. J. Pitts, J. Wityak, J. M. Smallheer, A. E. Tobin, J. W. Jetter, J. S. Buynitsky, P. P. Harlow, K. A. Solomon, M. H. Corjay, S. A. Mousa, R. R. Wexler, and P. K. Jadhav, "Isoxazolines as potent antagonists of the integrin alpha(v)beta(3).," *J. Med. Chem.*, vol. 43, pp. 27-40, 2000.
- [4] R. A. Mehl, J. C. Anderson, S. W. Santoro, L. Wang, A. B. Martin, D. S. King, D. M. Horn, and P. G. Schultz, "Generation of a bacterium with a 21 amino acid genetic code.," *J. Am. Chem. Soc.*, vol. 125, pp. 935-939, 2003.
- [5] J. Hugenholtz, W. Sybesma, M. N. Groot, W. Wisselink, V. Ladero, K. Burgess, D. van Sinderen, J. C. Piard, G. Eggink, E. J. Smid, G. Savoy, F. Sesma, T. Jansen, P. Hols, and M. Kleerebezem, "Metabolic engineering of lactic acid bacteria for the production of nutraceuticals," *Antonie Leeuwenhoek*, vol. 82, pp. 217-235, 2002.
- [6] K. Jain, "Lab-on-a-Chip and microarrays: discovery and development," *Pharmacogenomics*, vol. 4, pp. 123-125, 2003.
- [7] A. Pandey and M. Mann, "Proteomics to study genes and genomes," *Nature*, vol. 405, pp. 837-846, 2000.
- [8] D. S. Wilson and S. Nock, "Recent developments in protein microarray technology," *Angew. Chem. Int. Ed. Engl.*, vol. 42, pp. 494-500, 2003.
- [9] H. Zhu and M. Snyder, "Protein chip technology," *Curr. Opin. Chem. Biol.*, vol. 7, pp. 55-63, 2003.
- [10] R. W. Roberts and J. W. Szostak, "RNA-peptide fusions for the *in vitro* selection of peptides and proteins," *Proc. Natl. Acad. Sci. USA.*, vol. 94, pp. 12297-12302, 1997.
- [11] S. Weng, K. Gu, P. W. Hammond, P. Lohse, C. Rise, R. W. Wagner, M. C. Wright, and R. G. Kuimelis, "Generating addressable protein microarrays with PROfusion covalent mRNA-protein fusion technology," *Proteomics*, vol. 2, pp. 48-57, 2002.
- [12] S. Karamohamed, T. Nordstrom, and P. Nyren, "Real-time bioluminometric method for detection of nucleoside diphosphate kinase activity," *Biotechniques*, vol. 26, pp. 728-734, 1999.
- [13] I. Kienle, M. Burgert, H. Holzer, "Assay of trehalose with acid trehalase purified from *Saccharomyces cerevisiae*." *Yeast*, vol. 9, pp. 907-911 1993.
- [14] C. Schiraldi, I. Di Lernia, and M. De Rosa, "Trehalose production: exploiting novel approaches," *Trends Biotechnol.*, vol. 20, pp. 420-425, 2002.
- [15] H. Jorgensen, L. Olsson, B. Ronnow, and E. A. Palmqvist, "Fed-batch cultivation of baker's yeast followed by nitrogen or carbon starvation: effects on fermentative capacity and content of trehalose and glycogen," *Appl. Microbiol. Biotechnol.*, vol. 59, pp. 310-317, 2002.
- [16] Z. Chi, J. Liu, J. Ji, and Z. Meng, "Enhanced conversion of soluble starch to trehalose by a mutant of *Saccharomycopsis fibuligera* sdu," *J. Biotechnol.*, vol. 102, pp. 135-141, 2003.
- [17] M. A. Blázquez, R. Lagunas, C. Gancedo, and J. M. Gancedo, "Trehalose-6-phosphate, a new regulator of yeast glycolysis that inhibits hexokinases.," *FEBS Lett.* vol. 329, pp. 51-54, 1993.
- [18] J. M. Thevelein and S. Hohmann, "Trehalose synthase: guard to the gate of glycolysis in yeast?" *Trends Biochem. Sci.* vol. 20, pp. 3-10, 2002.
- [19] B. Teusink, M. C. Walsh, K. van Dam, and H. V. Westerhoff, "The danger of metabolic pathways with turbo design." *Trends Biochem. Sci.* vol. 23, pp. 162-169, 2002.
- [20] H. Kacser and L. Acerenza, "A universal method for achieving increases in metabolite production," *Eur. J. Biochem.*, vol. 216, pp. 361-367, 1993.